



RESEARCH ARTICLE

INFRARED AND DIELECTRIC PROPERTIES OF NICKEL ALUMINIUM FERRITE

*Singh, H. S. and Neha Sangwa

Department of Physics, J. N. V. University, Jodhpur, Rajasthan, India

ARTICLE INFO

Article History:

Received 08th December, 2017

Received in revised form

26th January, 2018

Accepted 17th February, 2018

Published online 28th March, 2018

Key words:

Nickel Aluminium Ferrite;
HEBM; FTIR, dielectric parameters.

ABSTRACT

Nickel Aluminium ferrite with general formula $NiAl_xFe_{2-x}O_4$ for 'x = 0.0, 0.2, 0.4, 0.6, 0.8 and 1.0' were synthesized by High Energy Ball milling. Fourier Transform Infrared Spectra (FTIR) and Dielectric characteristics were measured at room temperature as a function of frequency for synthesized ferrite. Infrared spectra exhibit two vibrational bands; high frequency band ν_1 observed for the samples in the range of 603 cm^{-1} to 632 cm^{-1} assigned by stretching vibrations of tetrahedral metal oxygen bond and low frequency band ν_2 observed in range 418 cm^{-1} to 489 cm^{-1} assigned due to metal oxygen vibrations in octahedral B sites. The dielectric investigation of Nickel Aluminium ferrite shows that the value of dielectric constant, dielectric loss and dielectric loss tangent are high at low frequency and become frequency independent at high frequencies.

Copyright © 2018, Singh and Neha Sangwa. This is an open access article distributed under the Creative Commons Attribution License, which permits unrestricted use, distribution, and reproduction in any medium, provided the original work is properly cited.

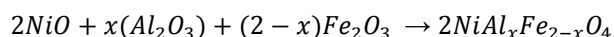
Citation: Singh and Neha Sangwa, 2018. "Infrared and dielectric properties of nickel aluminium ferrite", *International Journal of Current Research*, 10, (03), 66318-66322.

INTRODUCTION

Ferrites have been extensively studied and investigated enormously by many researchers in the recent decades due to their wide technological application in the present era. These technologically important materials were synthesized about 60 years ago (Valenzuel Raül, 2012). The nano sized ferrites materials have different physical properties as compared to those with bulk materials. In spinel ferrite family Nickel ferrite is the most important material with typical inverse spinel structure. The substitution of impurity in place of divalent ion or Fe^{3+} ion in pure nickel ferrite leads to the modification of the structural, electrical and magnetic properties of ferrite. The cations of the doped impurity get occupied in tetrahedral or octahedral sites and alter the dielectric properties. Substitution in Nickel ferrite makes it a good contender for the application as low loss materials at high frequencies (Singh and Neha Sangwa, 2015). The Infrared and dielectric analysis results for the Nickel Aluminium ferrite synthesized by High Energy Ball Mill are discussed in this paper.

Experimental details

Nickel Aluminium ferrite was prepared using Ball milling technique (Singh and Neha Sangwa, 2017). The solid state reaction is given as



*Corresponding author: Singh, H. S.

Department of Physics, J. N. V. University, Jodhpur, Rajasthan, India.

Fourier Transform Infrared Spectra (FTIR) of the prepared powder samples were recorded on a Bruker Vertex 70v spectrometer in the range of $400 - 4000\text{ cm}^{-1}$ with KBr as the reference sample. Measurements were performed in the transmission mode with spectroscopic grade KBr pellets. The dielectric parameters i.e. dielectric constant (ϵ), dielectric loss (ϵ'') and dielectric loss tangent ($\tan \delta$) were obtained by measuring the capacitance of the prepared sample powder using Solartron Impedance / Gain - Phase Analyser SI - 1260.

RESULTS AND DISCUSSION

Fourier Transform Infrared Spectroscopy for the synthesized samples of Nickel Aluminium ferrite nanoparticles were performed at room temperature in the spatial frequency range 400 to 4000 cm^{-1} . Figure 1 represents the infrared spectra for various composition of Aluminium 'x' in $NiAl_xFe_{2-x}O_4$. Infrared spectra found to exhibit two vibrational bands; high frequency band ν_1 observed for the samples around 600 ranges from 603 cm^{-1} to 632 cm^{-1} assigned by stretching vibrations of tetrahedral metal oxygen complexes and low frequency band ν_2 observed around 400 cm^{-1} for the samples ranges from 418 cm^{-1} to 489 cm^{-1} assigned due to metal oxygen vibrations in octahedral B sites (Battoo *et al.*, 2009). Difference in the frequency of two bands ν_1 and ν_2 are attributed due to the differences in the $Fe^{3+}-O^{2-}$ bond length at tetrahedral A sites and octahedral B sites (Mohammeda, 2012). The investigated values of low frequency band and high frequency band position are tabulated in Table 1. As the Aluminium concentration 'x' increases in $NiAl_xFe_{2-x}O_4$ the absorption bands ν_1 and band ν_2 of infrared spectra are observed to shift towards high frequency region. This occurs due to decrease in

lattice constant (Singh and Neha Sangwa, 2017) resulting in shrinking of unit cell. The force constant of the ions at tetrahedral A sites (K_t) and octahedral B sites (K_o) for infrared spectra frequency bands ν_1 and ν_2 are evaluated using the formula given as

$$K_{o/t} = 4 \pi^2 c^2 \nu_{1/2}^2 m$$

Where ‘ c ’ is the speed of light ($\approx 2.99 \times 10^{10}$ cm/s), ν is the vibrational frequency of tetrahedral and octahedral sites and m is the reduced mass of the Fe^{3+} and O^{2-} ions ($\approx 2.061 \times 10^{-23}$ g) (Bouhadouza *et al.*, 2015).

Table 1: Absorption bands (ν_1 and ν_2) force constant (K_o and K_t) for $NiAl_xFe_{2-x}O_4$ ferrite, nanoparticles for varying ‘ x ’

Comp. (x)	ν_1 (cm ⁻¹)	ν_2 (cm ⁻¹)	$K_t \times 10^5$ (dyne/cm)	$K_o \times 10^5$ (dyne/cm)
0.0	603.01	418.65	2.6450	1.2749
0.2	610.09	433.37	2.7074	1.3661
0.4	612.41	439.19	2.7281	1.4030
0.6	622.15	447.55	2.8155	1.4570
0.8	628.82	452.45	2.8762	1.4890
1.0	632.02	489.47	2.9056	1.7427

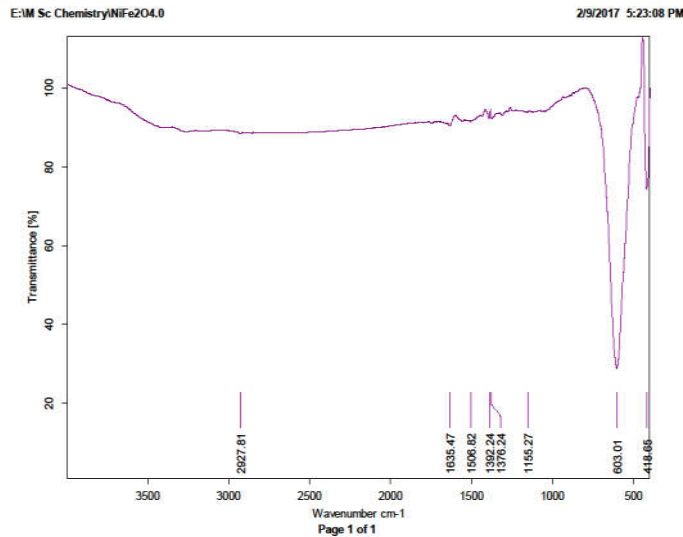


Figure 1. (a)

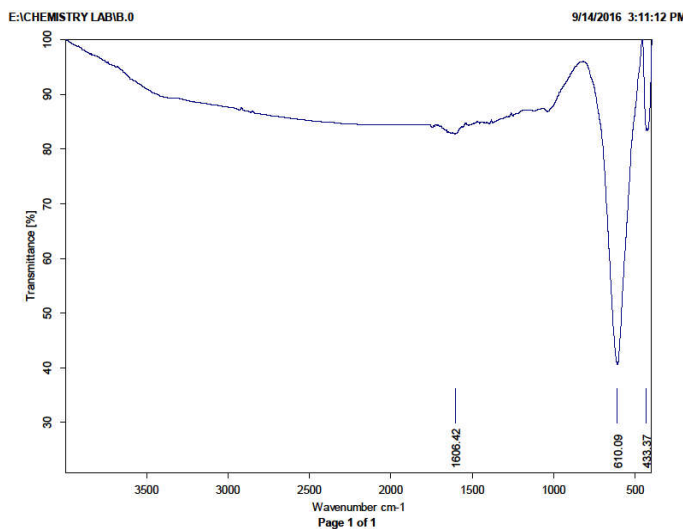


Figure 1. (b)

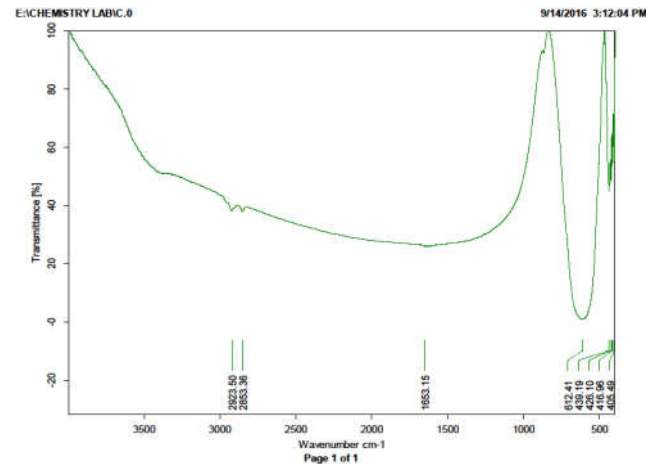


Figure 1. (c)

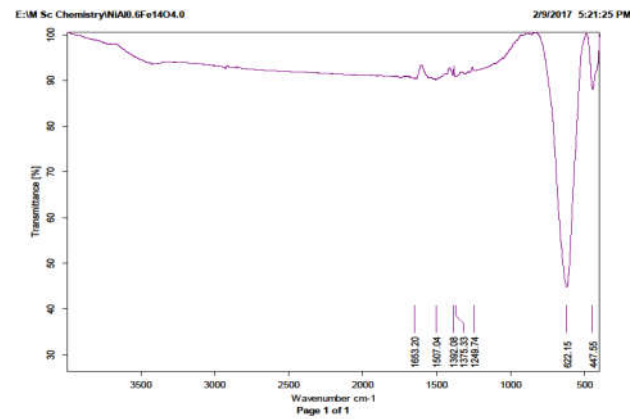


Figure (d)

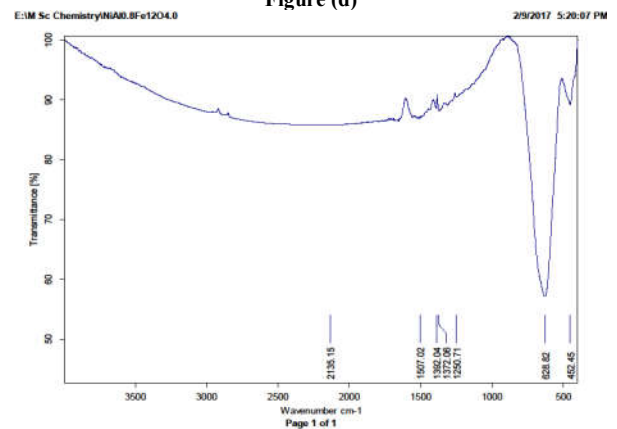


Figure 1. (e)

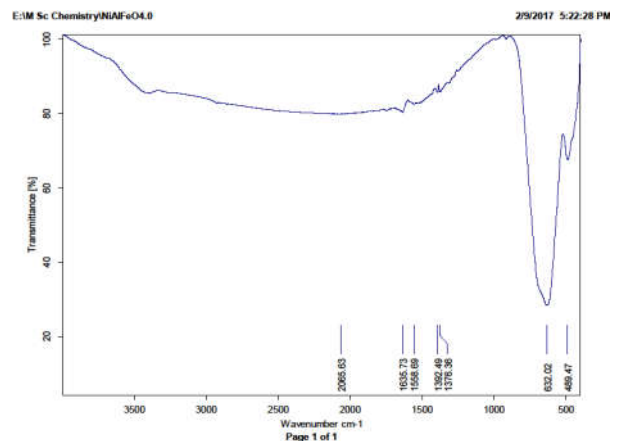


Figure 1. (f)

Figure 1. FT-IR spectra of $NiAl_xFe_{2-x}O_4$ for (a) $x = 0.0$, (b) $x = 0.2$, (c) $x = 0.4$, (d) $x = 0.6$, (e) $x = 0.8$ and (f) $x = 1.0$.

The values for force constant (K_t and K_o) are observed to increase with increasing Aluminium content 'x' in Nickel Aluminium ferrite as mentioned in Table 1. It can be interpreted that for longer bond length i.e. for octahedral B sites the force constant is less as compared to the shorter bond length at tetrahedral A sites (Singh and Neha Sangwa, 2017). Similar behaviour is reported for Mg-Zn ferrites (Mohammeda *et al.*, 2012), Ni-Zn ferrite (Birajdar *et al.*, 2012) and Co substituted ferrite (NicaValentin *et al.*, 2013). The results are in good agreement with the results of previous researches for Nickel ferrite (Kamellia Nejati and Rezvanh Zabih, 2012) and Nickel Aluminium ferrite (Bouhadouza *et al.*, 2015; Bhosale and Chougule, 2006; Patange *et al.*, 2013). The dielectric investigation of Nickel Aluminium ferrite shows that the value of dielectric constant, dielectric loss and dielectric loss tangent are high at low frequency and become frequency independent at high frequencies. The variation of dielectric constant and dielectric losses can be explained on the basis of space charge polarization due to inhomogeneous dielectric structure of the synthesized ferrite material (Mytil Khan and John Zhang, 2001; Raghavender and Jadhav, 2009). The decrease in dielectric constant and dielectric loss from low frequency region to high frequency region and attaining a constant value at high frequency is the general behaviour of all ferrites samples (Adeen, 1999). This type of dielectric dispersion can be explained on the basis conformity of Koop's theory (Koops, 1951) in agreement with Maxwell Wagner type interfacial polarization (Wagner and Heilman, 1993; Smith and Wijn, 1959). According to Maxwell Wagner model there are highly conducting grains present in poorly conducting grain boundaries in ferrite structure (Wagner and Heilman, 1993; Maxwell, 1973), that cause charges to accumulate between the interface of grain and grain boundaries. Figure 2 shows the variation of dielectric constant, dielectric loss and dielectric loss tangent with respect to frequency in range 100 Hz to 1 MHz. All sample with varying Aluminium composition 'x' shows dispersion with frequency.

Electron exchange phenomenon between Fe^{2+} and Fe^{3+} , results in local displacement of electrons in the direction of applied field, which determines the polarization in ferrites. Dielectric parameters have high value at low frequency due to the fact that on the application of alternating electric field electrons pile up at poorly conducting grain boundary as they reach there. This is the reason for occurrence of space charge polarization. As the frequency increases the electron exchange between Fe^{2+} and Fe^{3+} cannot follow the alternating electric field which reduces surface charge polarization and it gets eliminated (Smith and Wijn, 1959; Ravikumar *et al.*, 2012; Patange *et al.*, 2011). At high frequency charge carriers do not get sufficient time to change their orientation in accordance with the applied external alternating field (Koops, 1951; Naveen Kumari, 2015). As a result electrons reverse their direction with the increasing frequency of external applied alternating electric field thereby reducing the electron exchange at grain boundaries. Therefore a decrease in polarization takes place that makes the dielectric parameters i.e. dielectric constant and dielectric loss to have approximately constant values as observed at high frequencies.

The variation of dielectric constant and dielectric loss in accordance with the compositional variation of Aluminium in Nickel Aluminium ferrite nanoparticles investigated at room temperature at frequency 100 Hz and 1 MHz are shown in figure 3(a) and figure 3(b). The dielectric parameters ϵ and ϵ' decreases with the increasing concentration of Aluminium 'x'

in Nickel Aluminium ferrite nanoparticle samples. Al^{3+} ions highly prefer the octahedral B sites of ferrite structure (Abdeena *et al.*, 2002; Maxwell and Pickart, 1953). So, concentration of Fe^{3+} ions at octahedral B sites decreases gradually with increasing Aluminium concentration in Nickel Aluminium ferrite. The reduction of the Fe^{3+} ions on octahedral B sites slow down the electron transfer between Fe^{2+} and Fe^{3+} ions and hence decreases the polarization thereby reducing the values of dielectric parameters ϵ and ϵ' with increasing Al^{3+} concentration.

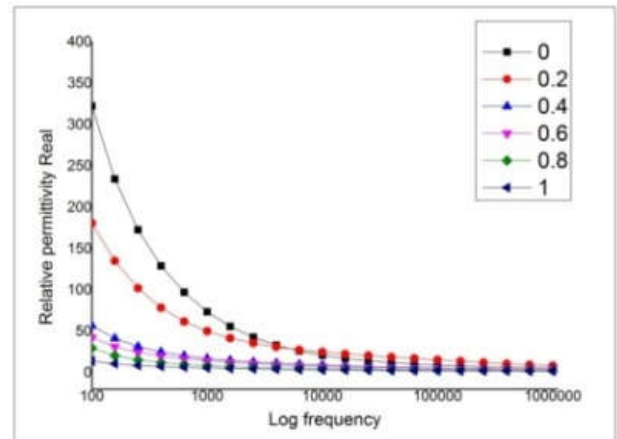


Figure 2(a)

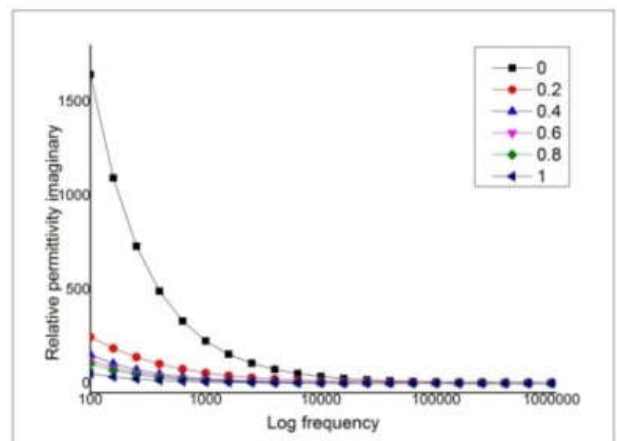


Figure 2(b)

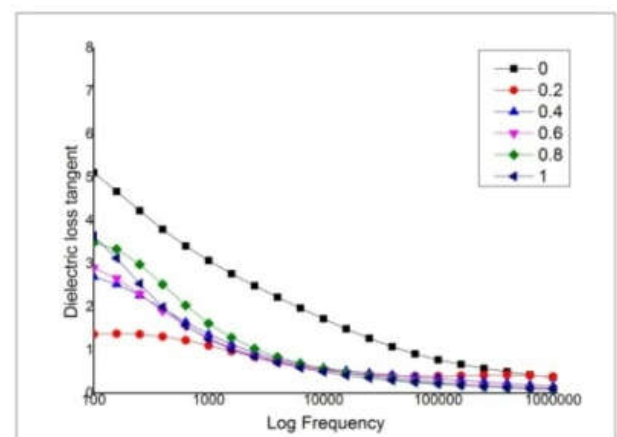


Figure 2(c)

Figure 2. Variation of (a): Dielectric constant (ϵ), (b): Dielectric loss (ϵ'') and (c): Dielectric loss tangent ($\tan \delta$) with logarithm of frequency For Nickel Aluminium ferrite

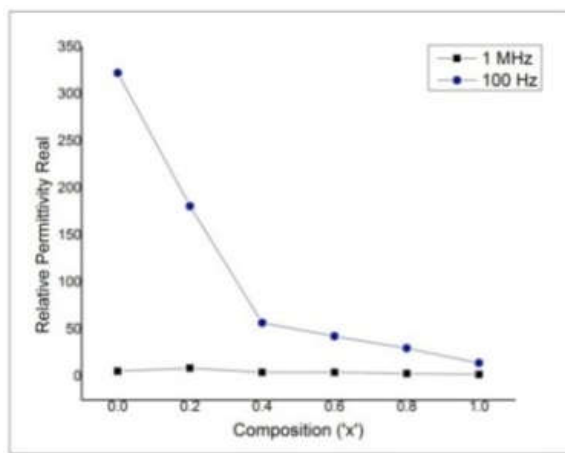


Figure 3(a)

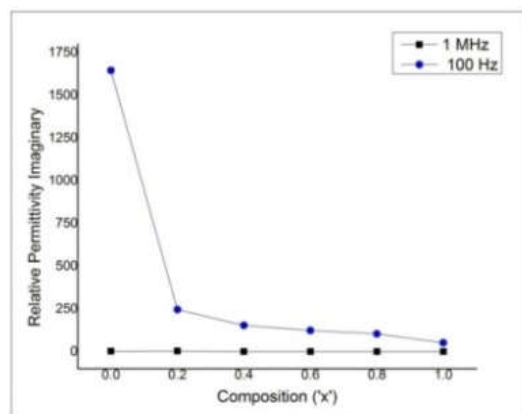


Figure 3(b)

Figure 3. Variation of (a): Dielectric constant (ϵ') and (b): Dielectric loss (ϵ'') with Aluminium composition 'x' at 100 Hz and 1 MHz for Nickel Aluminium Ferrite

Conclusion

Fourier Transform Infrared Spectra exhibit two vibrational bands near 600 cm^{-1} and 400 cm^{-1} shows the metal oxygen vibrational complexes in ferrite. The dielectric investigation represents that the reduction of the Fe^{3+} ions on octahedral B sites slow down the electron transfer between ferrous and ferric ions that concludes the decrease in polarization. The value of dielectric constant, dielectric loss and dielectric loss tangent are high at low frequency and become frequency independent at high frequencies. Increasing Aluminium concentration in Nickel Aluminium ferrite reduces dielectric parameters ϵ' , ϵ'' and $\tan \delta$. Ball Milling technique proves to be a good synthesis technique at industrial level.

Acknowledgement

The authors acknowledges for the financial support to UGC-BSR. The authors are thankful to DLJ DRDO for providing the facility for Dielectric characterization facility and IIT Jodhpur for providing FTIR characterization facility.

REFERENCES

Abdeena, A. M., Hemeddaa, O. M., Assem, E. E., EL-Sehly and M. M. 2002. "Structural electrical and transport

- phenomena of Co ferrite substituted by Cd", *J. Magn. Magn. Mater.*, 238, pp. 75-83.
- Adeen, A. M. 1999. "Dielectric behaviour in Ni-Zn ferrites", *J. Magn. Magn. Mater.*, 192, pp. 121-29,
- Batoo, K. M., Kumar Lee, S. and Alimuddin, C. G. 2009. "Study of dielectric and a.c. impedance properties of Ti doped Mn ferrites", *Curr. Appl. Phys.*, 9, 1397-06,
- Bhosale, A. G. and Chougule, B. K. 2006. "X-ray, infrared and magnetic studies of Al-substituted Ni ferrites", *Matr. Chem. and Phys.*, 97, pp. 273-76,
- Birajdar, A. A., Shirsath Sagar, E., Kadam, R. H., Mane, M. L., Mane, D. R. and Shitre, A. R. 2012. "Permeability and magnetic properties of Al^{3+} substituted $Ni_{0.7}Zn_{0.3}Fe_2O_4$ nanoparticles", *J Appl. Phys.*, 112, pp. 053908,
- Bouhadouza, N., A., Rais, S., Kaoua, M., Moreau, K. and Taibi, A. 2015. Addou, "Structural and Vibrational studies of $NiAl_xFe_{2-x}O_4$ ferrites ($0 \leq X \leq 1$)", *Cera. Int.*, 41, 11687-92.
- Kamellia Nejati and Rezvanh Zabih, 2012. "Preparation and magnetic properties of nano size nickel ferrite particles using hydrothermal method", *Chem. Central J.*, 23,
- Koops, C. G. 1951. "On the dispersion of resistivity and dielectric constant of some semiconductors at audio frequencies", *Phys. Rev.*, 83, 121,
- Maxwell L. R. and Pickart, S. J. 1953. "Magnetization in Nickel Ferrite-Aluminates and Nickel Ferrites Gallates", *Phys. Rev.*, 92, pp. 1120,
- Maxwell, J. C. 1973. "Electricity and Magnetism", Oxford University Press, London,
- Mohammeda, K. A. Al., Rawas, A. D., Gismelseed, A. M. and Sellai, M. 2012. A. Widatallah, H. M. Yousif, A. Elzain M. E. and Shongwe, "Infrared and structural studies of $Mg_{1-x}Zn_xFe_2O_4$ ferrites", *Physica*, B, 407, 795-04,
- Mytil Khan, L. and John Zhang, Z. 2001. "Synthesis and magnetic properties of $CoFe_2O_4$ spinel ferrite nanoparticles doped with Lanthanide ions", *Appl. Phys. Lett.* 78, 365,
- Naveen Kumari, Vinod Kumar and S. K. Singh, 2015. "Structural, dielectric and magnetic investigations on Al^{3+} substituted Zn-ferrospinel", *RSC Advances Publishing*,
- NicaValentin, Daniel Gherca, Ursu Cristian, Tudorache Florin, Brinza Florin and Pui Aurel, 2013. "Synthesis and Characterization of Co substituted ferrite Nanocomposites", *IEEE Transactions on Magnetics*, 49 (1),
- Patange, S. M., Sagar, E., Shirsath, K. S., Lohar, S. S., Jadhav, Kulkarni, N. and Jadhav, K. M. 2011. "Electrical and switching properties $NiAl_xFe_{2-x}O_4$ ferrites synthesized by chemical method", *Phys. B*, 406, pp.663,
- Patange, S. M., Sagar, E., Shirsath, S. P., Jadhav, V. S., Hogade, S. R., Kamble, K. M. and Jadhav, 2013. "Elastic properties of nanocrystalline aluminium substituted nickel ferrites prepared by coprecipitation method", *J. of Mole. Stru.*, 1038, pp.40-44,
- Raghavender, A. T. and Jadhav, K. M. 2009. "Dielectric properties of Al-substituted Co ferrite nanoparticles", *Bull. Mater. Sci.*, 32(6), pp. 575-78,
- Ravikumar, G., Vijayakumar, K. and Venudhar, Y. C. 2012. "Electrical Conductivity and Dielectric Properties of Copper Doped Nickel Ferrites Prepared by Double Sintering Method", *Int. J. of Mor. Engg. Res.*, 2(2), pp. 177-185,
- Singh H.S. and Neha Sangwa, 2015. "Review Article: Nickel Aluminium ferrite", *Int. J. of Sci. and Engg. Res.*, 6, pp. 765-768,

- Singh H.S. and Neha Sangwa, 2015. "Structural and Magnetic Properties of Nickel Ferrite Nanoparticles synthesized by Ball Milling", *Int. J. of Engg. Sci. Inve*, 6, pp. 36-39,
- Singh H.S. and Neha Sangwa, 2017. "Structural analysis of Aluminium substituted nickel ferrite nanoparticles", *Amer. Inst. of Phys*, Proceeding, under process November.
- Smith, J. and Wijn, H. P. J. 1959. "Ferrites—Physical Properties of Ferromagnetic Oxides in Relation to their Technical Applications", *Wiley New York*.
- Valenzuel Raúl, 2012. "Review Article: Novel Application of Ferrites", *Physics Research Int.*,
- Wagner K. W. and Heilman, E. L. 1993. "The distribution of relaxation times in typical dielectrics", *Ann. Phys*, 40, pp. 818.
